Engineering Structures 125 (2016) 349–363

Contents lists available at ScienceDirect

Engineering Structures

journal homepage: www.elsevier.com/locate/engstruct

Life-cycle cost and seismic reliability analysis of 3D systems equipped with FPS for different isolation degrees

P. Castaldo *, B. Palazzo, P. Della Vecchia

Dept. of Civil Engineering, University of Salerno, Via Giovanni Paolo II, 84084 Fisciano, SA, Italy

ARTICLE INFO

Article history:
Received 31 October 2015
Revised 21 May 2016
Accepted 30 June 2016
Available online 25 July 2016

Keywords:
Isolation degree
Life-cycle cost analysis
Seismic reliability
FP bearings
Structural performance
Joint PDF

ABSTRACT

The aim of the study consists in evaluating the life-cycle costs of a r.c. 3D system isolated by single-concave FPS bearings with different isolated periods in order to evaluate the potential benefits provided by increasing values of the isolation degree. In particular, assuming the elastic response pseudo-acceleration related to each isolated period and the coefficient of friction as random variables relevant to the problem characterized by appropriate probability density functions, the Latin Hypercube Sampling method has been adopted as random sampling technique in order to define the input data and perform 3D non-linear dynamic analyses. Thus, bivariate structural performance curves for each story of the superstructure and for the substructure as well as seismic reliability-based design (SRBD) abacuses for the isolation level have been defined for the different values of the isolation degree. Finally, the life-cycle cost analysis of the isolated system with different curvature radius of the FP bearings has been accomplished taking into account both the initial costs and the expected loss costs, due to future earthquakes, of the overall system during its design life (50 years) in order to evaluate the influence of the isolation degree on both the seismic performance and the total costs.

1. Introduction

Seismic isolation through friction pendulum system (FPS) devices represents a widely used and effective technique for the seismic protection of buildings, bridges and industrial structures [1,2]. Many advantages can be achieved by employing such kind of frictional isolators respect to elastomeric bearings as discussed in [3–5]. Over the years, several research works have been focused on probabilistic analyses, structural reliability methods and reliability-based analysis [6,7] by evaluating the stochastic responses of base-isolated structures under random earthquake excitations. Reliability evaluation of base-isolated systems has been presented by Chen et al. [7] as well as Monte Carlo simulations have been performed by Fan and Ahmadi [8] and Su and Ahmadi [9] to analyze the stochastic response of sliding isolation systems under random earthquake excitations. Many studies have also dealt with reliability analysis and reliability-based optimization of base-isolated systems including uncertainties such as isolation device properties and ground motion characteristics [10–13].

The influence of the friction pendulum system (FPS) isolator properties on the seismic performance of base-isolated building frames by employing a two-degree-of-freedom model accounting for the superstructure flexibility with a velocity-dependent model for the FPS isolator behaviour has been analyzed in [14]. The variation of the statistics of the response parameters relevant to the seismic performance has been investigated through the nondimensionalization of the motion equation considering different isolator and system properties and the results can be used for deriving approximate fragility curves and for simplified seismic risk analyses.

Seismic reliability analyses of a r.c. 3D system isolated by FPS bearings with a design life of 50 years and located near L'Aquila site (Italy) have been carried out in Palazzo et al. [15,16] and Castaldo et al. [17] by accounting for the randomness of both the isolator properties and earthquake main characteristics. Monovarite and bivariate structural performance (SP) curves for the isolator and the superstructure have been estimated and compared to the results obtained following the PEER-like modular approach [18], usually employed in seismic risk and reliability analyses, confirming the effectiveness of the derived structural reliability curves. This way, a reliability criterion has been defined to assist the design of the isolator dimensions in plan by considering the effects of the uncertainties relevant to the problem and demonstrating the importance of considering the bivariate exceeding probabilities

* Corresponding author.
E-mail addresses: pcastaldo@unisa.it (P. Castaldo), palazzo@unisa.it (B. Palazzo), dellavecchiapasquale@gmail.com (P. Della Vecchia).

http://dx.doi.org/10.1016/j.engstruct.2016.06.056
0141-0296/

Nomenclature

a	sliding velocity transition rate parameter of the FPS
C_{IN}	initial construction cost
C_{LS}	limit states dependent cost in the design-life time
$C^{i}_{LS,s}$	ith structure limit state dependent cost in the design-life time
$C_{LS,d}$	FPS limit state dependent cost in the service life of the isolator
F	FPS restoring force
$f_{\max}$	sliding coefficients of friction at large velocity of the FPS
$f_{\min}$	sliding coefficients of friction nearly zero velocity of the FPS
g	gravity acceleration
I_d	isolation degree
K_{eff}	FPS isolator effective stiffness at the displacement design
K_1	FPS elastic stiffness
K_2	FPS post elastic stiffness
M	mass on the bearing
M_x	bending moment around the x axis
M_y	bending moment around the y axis
M	magnitude
N	number of limit state dependent cost
q	reduction factor
P	axial force
P_i	exceedance probability of the ith damage state given an earthquake occurrence
P_f	exceeding probability in 50 years
$P(\Delta > \Delta_i)$	lifetime exceedance probability of the ith limit state Δ_i
$P_{t=1}(\Delta > \Delta_i)$	annual exceeding probability of the ith limit state Δ_i
Q_d	FPS characteristic strength
r	radius in plan of the FPS
R	radius of curvature of the FPS
R	epicentral distance
S_a	elastic pseudo-acceleration
sgn	signum function of the sliding velocity
T_{eff}	effective period of vibration of the base-isolated system at the displacement design
T_{fb}	first natural period of the fixed-base structure
T_{is}	fundamental period of vibration of the base-isolated system
u_d	design displacement of the FPS
$\dot{u}$	sliding velocity of the FPS
u	absolute maximum bivariate horizontal relative displacement of the FPS
u_x	absolute maximum horizontal relative displacement along x direction of the FPS
u_y	absolute maximum horizontal relative displacement along y direction of the FPS
W	weight on the bearing
W_s	total weight of superstructure and isolation level
α	mass proportional coefficient related to Rayleigh damping
β	reliability index
β	stiffness proportional coefficient related to Rayleigh damping
δ	absolute maximum bivariate interstory drift
δ_x	absolute maximum interstory drift along x direction
δ_y	absolute maximum interstory drift along y direction
Θ	rotational degree of freedom of the 3D building around vertical axis
λ	annual monetary discount rate
μ	sliding coefficient of friction of the FPS
ν	annual occurrence rate of significant earthquake
ξ_{eff}	FPS isolator effective damping at the displacement design
ξ_{is}	dimensionless damping coefficient of the base-isolated building

due to the three-dimensional effects and correlations between the plane response parameters.

With reference to the management of new and existing civil structures in earthquake engineering, a widely recognized assessment tool for the system performance estimation, capable to take also into account the potential damages due to future earthquakes, is based on the cost-effectiveness criterion as discussed by Ang and Lee [19]. This way, regarding a structure under seismic risk, an optimization of the design variables may be achieved through a tradeoff between the costs of protection systems versus potential future losses caused by earthquakes [20,21–23]. Thus, the cost-effectiveness criterion also represents a purpose in order to define the optimal integrated seismic design solutions of control systems and structures [24–26].

Within the cost-effectiveness based design, this work aims to further advance the study of Castaldo et al. [17] by evaluating the life-cycle costs of a r.c. 3D system isolated by single-concave FPS bearings with different isolated periods in order to evaluate the potential benefits provided for increasing values of the isolation degree [27,28]. In particular, assuming the elastic response pseudo-acceleration related to each isolated period and the coefficient of friction as the random variables relevant to the problem, characterized by appropriate probability density functions (PDFs) according to [29,30–32], respectively, the Latin Hypercube Sampling method (LHS) [33–36] has been adopted as random sampling technique in order to define the input data and perform 3D nonlinear dynamic analyses. For each dynamic analysis, the three dimensional components of each seismic event and the nonlinear behaviour of the superstructure, designed in full compliance with NTC08 [29], have been considered. Thus, bivariate structural performance (SP) curves for each story of the superstructure and for the substructure as well as seismic reliability-based design (SRBD) abacuses for the isolation level have been defined for the different values of the isolation degree. Finally, the life-cycle cost analysis (LCCA) [37–39] for the different configurations of the isolated system with various curvature radius of the FP bearings has been accomplished taking into account both the initial costs and the expected loss costs, due to future earthquakes, of the overall system during its design life (50 years) in order to evaluate the influence of the isolation degree on both the seismic performance and the total costs.

2. Life-cycle cost analysis (LCCA) of base-isolated systems

Within the life-cycle cost analysis (LCCA) of a base-isolated (BI) structure, the cost-effectiveness criterion is based on the computation of the costs related to both the protection system (including substructure, superstructure and isolation devices) and potential losses caused by future earthquakes during its design life and, as suggested by [20–23], may be useful to achieve an optimization of the design variables.

The total expected life-cycle cost [19,37] of a BI structure is assumed to be the sum between the initial construction cost C_{IN}

Table 1
Limit state dependent cost calculation formula [38].

Cost Category	Calculation formula	Basic cost	
C_1 - *Damage*	Replacement cost × floor area × mean damage index	1500	MU/m^2
C_2 - *Loss of content*	Unit contents cost × floor area × mean damage index	500	MU/m^2
C_3 - *Rental*	Rental rate × gross leasable area × loss of function	10	MU/month/m^2
C_4 - *Income*	Rental rate × gross leasable area × down time	2000	MU/year/m^2
C_5 - *Minor Injury*	Minor injury cost per person × floor area × occupancy rate × expected minor injury rate	2000	MU/person
C_6 - *Serious Injury*	Serious injury cost per person × floor area × occupancy rate × expected serious injury rate	2.00E+04	MU/person
C_7 - *Human death*	Human fatality cost per person × floor area × occupancy rate × expected death rate	2.80E+06	MU/person

Occupancy rate 2 person/100 m^2.

and the present value of the lifetime limit states dependent cost C_{LS} as expressed in Eq. (1):

$$C_{TOT} = C_{IN}(\boldsymbol{s}) + C_{LS}(t, \boldsymbol{s}) \tag{1}$$

where t is the design-life time period of the structure, $\boldsymbol{s}$ is the design vector composed of the structural parameters influencing the performance of the structural system (i.e., isolation degree I_d), $C_{IN}(\boldsymbol{s})$ is the initial construction cost and $C_{LS}(t, \boldsymbol{s})$ represents the limit states dependent cost, also defined as the cumulative damage cost in present value, including direct damage cost and indirect loss under all earthquakes that could occur over the life of the structure.

The initial construction cost $C_{IN}(\boldsymbol{s})$ takes into account for (i) initial and regular maintenance cost of the isolation devices and (ii) initial system (superstructure and substructure) construction cost. The initial cost of the isolation devices is defined on the basis of the radius in plan r of the concave surface of the FPS bearings required to respect the target reliability level (or the target exceeding probability related to the collapse state, i.e., equal to $P_f = 1.5 \cdot 10^{-3}$ for a design life of 50 years) as obtained from the $SP_{isolator}$ curves derived within the seismic reliability analysis. The regular maintenance replacement cost of the isolation devices is the cost of their replacement after 10 years service life, required as minimum value in the preventive hypothesis that the devices are not able to respect the recommendations provided from the maintenance plans according to [29]. The initial system (superstructure and substructure) construction cost is assumed to be proportional to the initial FP bearings cost being the influence of the isolation system cost on the construction cost of an ordinary building equal to about 5–10% [40].

The limit states dependent cost $C_{LS}(t, \boldsymbol{s})$ takes into account (i) special maintenance cost of isolation devices $C_{LS,d}$ and (ii) limit states cost of the structure (superstructure and substructure) depending on each limit state cost, $C^i_{LS,s}$, where i represents the ith limit state. The special maintenance cost of isolation devices is the present value of the cost required to replace the devices if the maximum allowable isolator displacement (radius in plan r) will be reached or exceeded due to the occurrence of the significant earthquakes considered. The limit state cost for the ith limit state on the superstructure and substructure is given by potential direct damage cost and indirect loss under the significant earthquake events that can occur during the design life of the system.

As for the limit states, the performance based-design framework, defined in SEAOC [41], focused the attention on four structural performance levels related to four damage levels on a structure, or limit states "*LS1*", "*LS2*", "*LS3*", "*LS4*", corresponding respectively to "fully operational", "operational", "life safety" and "collapse prevention". As recommended by FEMA-350 [42] and Ghobarah [43], the interstory drift is one of the most suitable performance criterion for r.c. frame structures. Therefore, the Interstory Drift Index, IDI, is considered in this study as the response measurable parameter to identify the performance of a r.c. structure within the code limit states. In Table 1, the cost categories with the corresponding calculation formulas and the basic costs, described in [38], are reported. Each one of these cost items is based on a damage index or expected rate data according to FEMA-227 [44] and ATC-13 [45].

In Table 2, regarding the abovementioned four limit states, the calculation indices and rates useful to define the limit states dependent cost of Table 1, defined according to FEMA-227 and ATC-13 provisions, are reported.

Therefore, the limit state cost for the ith limit state on the structure (superstructure and substructure) $C^i_{LS,s}$ can be expressed as follows:

$$C^i_{LS,s} = C^i_1 + C^i_2 + C^i_3 + C^i_4 + C^i_5 + C^i_6 + C^i_7 \tag{2}$$

where the value of each term on the right side is calculated as the product between the corresponding value reported in Table 1 and the relative indices and rates given in Table 2. The limit state dependent cost function of the overall system, considering (i) N limit states and assuming that (ii) the earthquake occurrence assessment is based on a Poisson process model and (iii) the building is immediately fully restored to its original condition after each damage, can be written as [37,38]:

$$C_{LS}(t, \boldsymbol{s}) = \frac{\nu}{\lambda}(1 - e^{-\lambda t}) \sum_{i=1}^{N} C^i_{LS,Sum} P_i \tag{3}$$

where

$$P_i = P(\Delta > \Delta_i) - P(\Delta > \Delta_{i+1}) \tag{4}$$

and

$$P(\Delta > \Delta_i) = -\frac{1}{\nu t} ln[1 - P_{t=1}(\Delta > \Delta_i)] \tag{5}$$

where $N = 4$ ("*LS1*", "*LS2*", "*LS3*", "*LS4*"), ν is the annual occurrence rate of the significant earthquake [38], modelled by a Poisson process, t is the design-life time period of the structure, $(1 - e^{-\lambda t})/\lambda$ gives the present value of the cumulative damage cost, λ is the annual monetary discount rate, considered equal to 5% [38,39], P_i is the probability of the ith damage state being violated given the earthquake occurrence, Δ_i and Δ_{i+1} are the lower and upper bounds of the ith limit state, $P(\Delta > \Delta_i)$ and $P_{t=1}(\Delta > \Delta_i)$ are the lifetime and annual exceeding probability of the ith limit state expressed in terms of the bivariate maximum interstory drift $\Delta_i = \delta_i$, as defined in the following sections.

The limit state special maintenance cost of isolation devices, $C_{LS,d}$, is the cost necessary to keep the original capability of the devices and can be expressed through Eq. (3) considering the only limit state, $i = 1$, for which the displacement demand results to be equal to the design displacement of the FPS isolators, $\Delta = u = r$, within the preventive hypothesis of considering the FPS service-life $t = 10$ years [29]. It follows that the term $C^i_{LS,Sum}$ of Eq. (3) is the cost of new devices.

Table 2
Limit states, interstory drift index, damage index, minor injury, serious injury and death rate, average loss of function and down time [17,44,45].

Limit state	BI structure interstory drift index (%) (FEMA 274) (NTC08)	FEMA 227				ATC 13	
		Mean damage index (%)	Expected minor injury rate	Expected serious injury rate	Expected death rate	Loss of function (%)	Down time (%)
LS1	0 < IDI < 0.1 0 < IDI < 0.2	5	0.0003	0.00004	0.00001	3.33	3.33
LS2	0.1 < IDI < 0.2 0.2 < IDI < 0.4	20	0.003	0.0004	0.0001	12.4	12.4
LS3	0.2 < IDI < 0.5 0.4 < IDI < 1.0	45	0.03	0.004	0.001	34.8	34.8
LS4	IDI > 0.7 IDI > 1.3	100	0.4	0.4	0.2	100	100

3. Structural models and uncertainties for the seismic reliability analysis

The evaluation of the limit state dependent cost for a BI building structure under random seismic loads requires the definition of its seismic reliability by computing the SP curves expressed in terms of the probabilities exceeding the maximum values of the engineering demand parameters (EDPs), expressed in terms of bivariate interstory drift δ for both substructure and superstructure and bivariate relative displacement u for the isolation level.

Within the seismic reliability, many code provisions [46,47] and guideline documents [41] are aimed at improving the seismic performances as well as to reduce damage costs under a certain level of earthquake risk without any compromise to the fundamental life-safety objective. As also discussed in [17], the four structural performance objective (PO) levels according to [41,48–51], are coupled with appropriate reliability indices β, or exceeding probability of the limit states, during the design life of the structure [46]. The considered limit states with the reliability indices as well as the maximum interstory drift limits related to a fixed-base (FB) structure and the maximum interstory drift limits, reduced according to both American [47] and Italian seismic code [29] provisions, for base-isolated (BI) systems are reported in Table 3. Fig. 1 illustrates the performance objective (PO) curves for fixed-base and base-isolated systems [17].

The assessment of the seismic reliability of a base-isolated structure is carried out by comparing the structural capacity of the building, structural performance (SP) curves, to the PO curves.

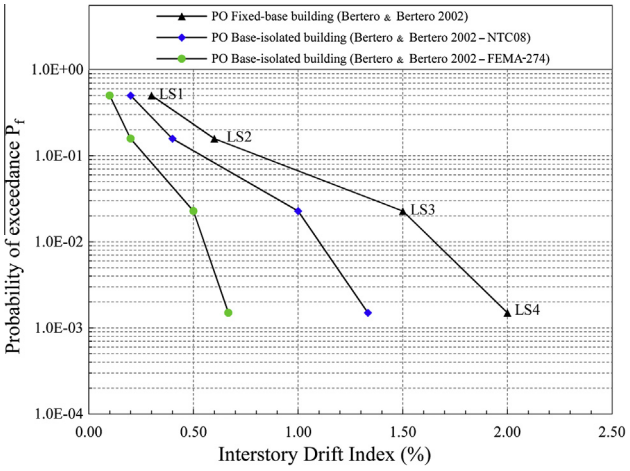

Fig. 1. Exceeding probability (in 50 years) corresponding to the performance limit states in the "performance space".

3.1. Structural models

Four different models of a r.c. 3D base-isolated building with a design life of 50 years have been considered in order to evaluate the influence of the isolation degree $I_d = (T_{is}/T_{fb})$, defined as the ratio between the isolated period T_{is} and fixed-base period T_{fb} [27,28], on both the seismic reliability and life-cycle costs of the overall system.

The four-story symmetric reinforced concrete 3D frame building, analyzed in similar studies [17,52], has been adopted in this work as benchmark building model. The superstructure and substructure, disconnected by the isolation level, are, respectively, composed of three (4th, 3rd, 2nd stories) and one (1st story) levels. The beams rectangular cross sections are the same in all stories and all frames, as well as all the superstructure and substructure columns have the same square cross section, respectively. The plan dimensions of the structure are 8.0 × 16.0 m with slabs having a depth of 0.40 m; the interstory height of the superstructure is 3.5 m; superstructure column section dimensions are 0.70 × 0.70 m, respectively; beam section dimensions are 0.40 × 0.70 m for each floor level. Story masses is amounted to 100 tons for each story, leading to a total seismic weight of the structure W_s = 512.0 tons. The substructure is composed of six columns having 0.80 × 0.80 m section dimension with a height equal to 3.0 m.

The four different base-isolated structural models (*SM*) have been designed by employing friction pendulum isolators with different radius of curvature R and considering a common low value of the sliding coefficient of friction μ = 3%: *SM1* (R = 1.5 m), *SM2* (R = 2.0 m), *SM3* (R = 3.0 m), *SM4* (R = 4.0 m).

The different structural models have been designed according to the Italian earthquake design requirements for base-isolated structures [29]. In fact, for each one of the four base-isolated models, considered to be located near L'Aquila site (geographic coordi-

Table 3
Limit states, reliability indices in 50 years, maximum fixed-base and base-isolated Interstory Drift Indices [17,49,51].

Limit state	Damage	FB IDI (%)	Reliability index β	P_f	BI structure (NTC 08) IDI (%)	BI structure (FEMA-274) IDI (%)
LS1	Slight	0 < IDI < 0.3	0	$5.0 \cdot 10^{-1}$	0 < IDI < 0.2	0 < IDI < 0.1
LS2	Moderate	0.3 < IDI < 0.6	1	$1.6 \cdot 10^{-1}$	0.2 < IDI < 0.4	0.1 < IDI < 0.2
LS3	Heavy	0.6 < IDI < 1.5	2	$2.2 \cdot 10^{-2}$	0.4 < IDI < 1.0	0.2 < IDI < 0.5
LS4	Collapsed	IDI > 2	3	$1.5 \cdot 10^{-3}$	IDI > 1.3	IDI > 0.7

nates 41°58′25″N, 13°24′00″E, Italy) on soil type B, the reinforcement bars of the structural members have been designed through the response spectrum analysis by employing the NTC08 response spectrum for an earthquake event with 475 years return period (corresponding to life safety limit state) and a reduction factor $q = 1.5$ [29]. Moreover, the non-linear behaviour of the single-concave isolation level has been taken into account, considering an equivalent linear behaviour [28,53] of the friction isolators estimating the effective stiffness K_{eff}, the corresponding effective period T_{eff} and effective damping ξ_{eff} as:

$$K_{eff} = W \cdot \left(\frac{1}{R} + \frac{\mu}{u_d}\right) \tag{6}$$

$$T_{eff} = \sqrt{\frac{1}{g\left(\frac{1}{R} + \frac{\mu}{u_d}\right)}} \tag{7}$$

$$\xi_{eff} = \frac{2}{\pi} \cdot \frac{1}{\frac{u_d}{\mu \cdot R} + 1} \tag{8}$$

where $W = M \cdot g$ is the weight on the bearing with mass M, g is the gravity acceleration, μ is the friction coefficient selected equal to 0.03 and u_d is the horizontal design displacement of the FPS bearing. The superstructure results to be characterized by a post-yield stiffness ratio higher than 3% in both directions. Provided the seismic hazard related to L'Aquila (Italy) is assumed, the life safety design

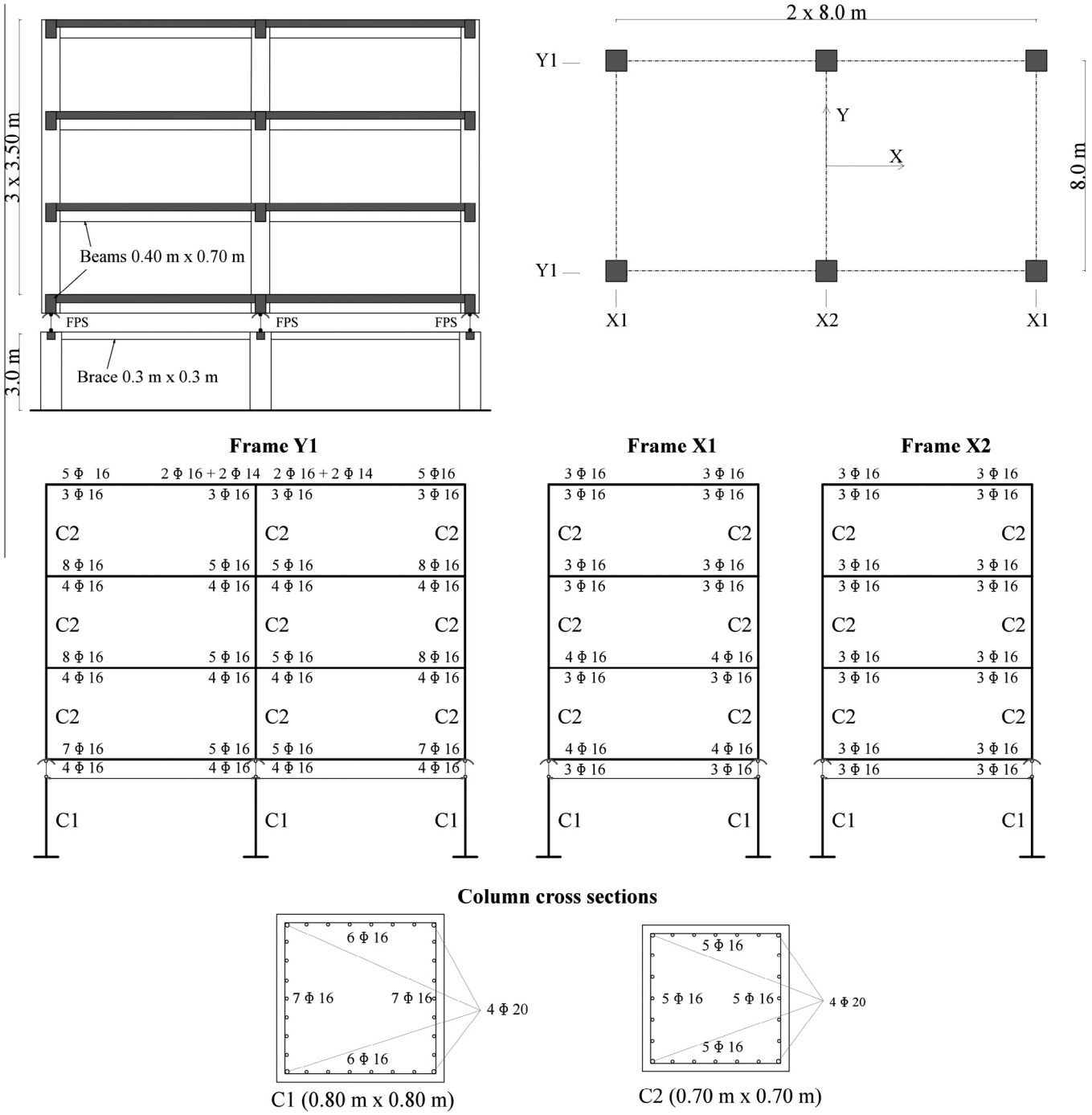

Fig. 2. Four-story base-isolated benchmark model: front and plan views; beams reinforcement bars; columns reinforcement bars.

is in compliance also with all the design and construction recommendations reported in [41,47] for the sliding coefficient of friction $\mu = 3\%$. Moreover, as for "*LS1*", "*LS2*" limit states, the stiffness of the frames is also adequate to respect the more restrictive plane and spatial requirements for base-isolated systems according to both [29,47] (Table 3 and Fig. 1) at each story.

A FEM model, Fig. 2, has been defined in SAP2000 [54] with the aim to perform 3D non-linear dynamic analyses considering the non-linear behaviour of the overall system (superstructure, substructure and isolation level). Each floor has been modelled as diaphragm and assumed to be rigid in its own plane, so that at each level three degrees of freedom resulted: two lateral degrees of freedom in the x and y directions, and a rotational degree of freedom (Θ) around the vertical axis.

As for the mechanical behaviour of the single-concave FPS isolation level, the force relative to a displaced position is defined by Eq. (9) [28]:

$$F = \mu W sgn(\dot{u}) + \frac{W}{R}u \tag{9}$$

in which, *sgn* denotes the signum function of the sliding velocity $\dot{u}$. In SAP2000 [54], the force–deformation behaviour of the FP isolator has been modelled through a non-linear hysteretic rule such as a bilinear model [17,28]. Three parameters, the characteristic strength Q_d given by $Q_d = \mu W$, the post-elastic stiffness determined as $K_2 = W/R$ and the elastic stiffness K_1, characterize the bi-linear hysteresis loop of the non-linear force deformation behaviour of the FP bearing. The characteristic strength, $Q_d = \mu W$, is related to the coefficient of friction and the weight on the bearing. The post-elastic stiffness of the isolation system, $K_2 = W/R$, is generally designed in such a way to provide the specific value of the isolation period $T_{is} = 2\pi\sqrt{M/K_2}$. The elastic stiffness K_1 should be at least 51 times larger than the post-elastic stiffness K_2, as defined in Naeim and Kelly [28]. The dependence of the friction μ on sliding velocity of the FPS isolators, as described in [14,17,55–57], has also been modelled as [30–32]:

$$\mu = f_{\max} - (f_{\max} - f_{\min})exp(-a\dot{u}) \tag{10}$$

where $f_{\max}$ and $f_{\min}$ are the sliding coefficients of friction at large velocity and nearly zero sliding velocity respectively. The rate parameter "*a*" equal to 50 s/m and a ratio between $f_{\max}$ and $f_{\min}$ equal to 3 have been selected according to the experimental data [30].

The elastic dynamic characteristics from the eigenvalue analysis of the different configurations are listed in Table 4. The first natural period of the fixed-base structure results being $T_{fb} = 0.58$ s, the period of the base-isolated model T_{is} ranges from 2.58 s to 4.01 s leading to values of the isolation degree I_d higher than 3 for all the configurations, as recommended in the Italian seismic code provisions [29] and in [58]. A Rayleigh damping model has been assumed and, setting a low value of the damping coefficient of the first two modes of the 3D base-isolated structure equal to $\xi_{is} = 2\%$ as suggested by [10,15–17,52], mass proportional α and stiffness proportional β coefficients result being equal to 0.0244 and 0.0041, respectively.

Table 4
Fixed-base and base-isolated structural models characteristics.

Structural model	T_{is} (s)	R (m)	$I_d = T_{is}/T_{fb}$
SM1	2.58	1.5	4.5
SM2	2.84	2.0	5.3
SM3	3.47	3.0	6.4
SM4	4.01	4.0	7.4

Fixed-base structural model period $T_{fb} = 0.58$ s.

As for the non-linear mechanical behaviour of the r.c. structural members implemented in SAP2000 [54], beam and column elements are modelled as non-linear frame elements with lumped plasticity defined according to [59]. Constitutive laws for the non-linear behaviour of the r.c. sections, suggested by the codes [59], are adopted without considering more complex approaches useful in specific cases [60,61]. For the column hinges the interaction between the axial force and the bending moments ($P\text{-}M_y\text{-}M_x$) has been taken into account, while the bending moments ($M_y\text{-}M_x$) interaction has been considered for the beams hinges.

3.2. Random variables

With the scope to perform the inelastic dynamic time-history analyses aimed at evaluating the seismic reliability of the 3D base-isolated structure, it is necessary to (i) define the source of uncertainties (random variables) relevant to the problem with the corresponding probability density functions (PDFs), (ii) choose an appropriate sampling method (Latin Hypercube Sampling method, LHS), (iii) generate the input data sets.

According to [15–17], the isolator sliding coefficient of friction and the ground motion intensity (i.e., elastic response accelerations at the isolated structural periods with a damping coefficient equal to 2%), are the two variables relevant to the system response to be considered as independent random variables. In fact, for regular systems, the superstructure characteristics, in terms of stiffness, mass and material properties, have not been included as random variables since they do not produce great effects on the statistical values of the response parameters of isolated systems, especially in the case of high values of the isolation degree, as discussed in Kulkarni and Jangid [62].

As for the uncertainty on the sliding friction coefficient, the experimental data developed by [30–32] on sheet type Teflon bearings, have pointed out that friction is a complex phenomenon, not complying with the Coulomb friction law (friction constant during sliding) and several mechanisms, such as (i) sliding velocity, (ii) normal load, (iii) temperature effects, (iv) number of cycles, contribute to its variability and can modify its statistical values under dynamic conditions showing a very high uncertainty within the range considered. Taking into account the above studies, a uniform probability density function in the range 0.03–0.15 is assumed to model the coefficient of friction $f_{\max}$ as random variable.

The uncertainty of ground motions has been taken into account, according to the probabilistic seismic hazard analysis (PSHA)

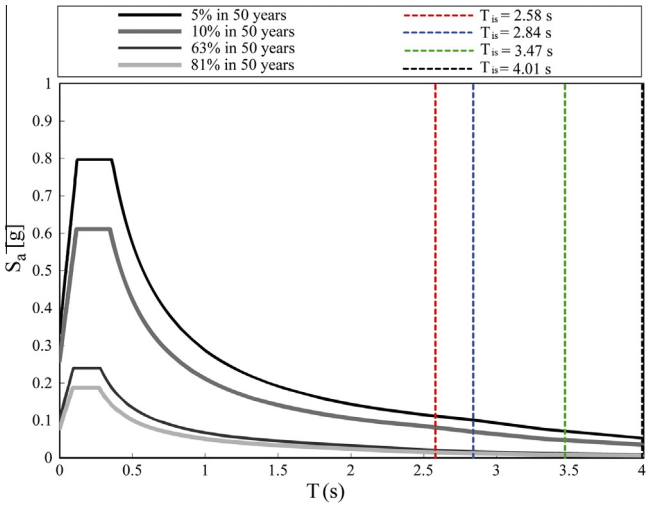

Fig. 3. Elastic pseudo-acceleration response spectra (in 50 years) ($\xi_{is} = 2\%$, coordinates 41°58′25″N, 13°24′00″E, Italy) [29].

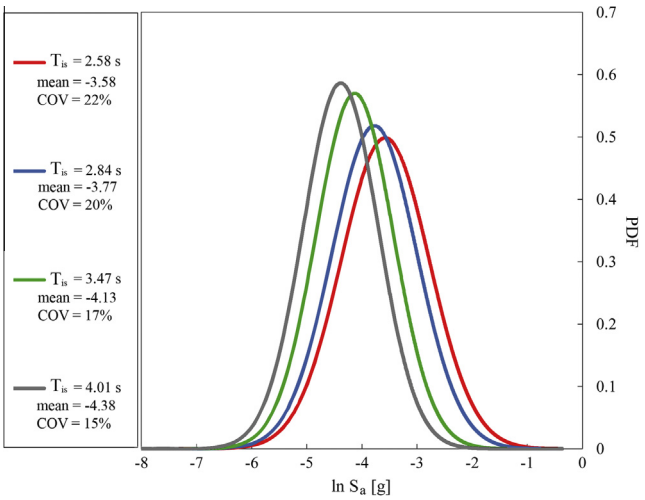

Fig. 4. PDFs of the seismic intensity measure lnS_a[g] (ξ_{is} = 2%) related to the BI structure periods.

[63,64], assuming the intensity measure (IM), $lnS_a(T_{is})$[g], as a random variable characterized by a Gaussian probability density function (PDF). The choice of an adequate IM should be driven by criteria of efficiency, sufficiency, and hazard computability [63,64]. As proposed in [17], the elastic response pseudo-accelerations at the isolated periods of the system, $S_a(T_{is})$ [g], are assumed as intensity measure according to [65,66]. For each Italian site and design life, the values of the abovementioned seismic intensity measure, related to the four limit states (*LS1*, *LS2*, *LS3*, *LS4*) with 50 years exceeding probabilities equal to 81%, 63%, 10% and 5% respectively, are provided by NTC08 [29]. Indeed, with reference to the location (geographic coordinates: 41°58′25″N, 13°24′00″E) near L'Aquila site (Italy), design life of 50 years and dimensionless damping coefficient equal to ξ_{is} = 2%, Fig. 3 shows the elastic acceleration response spectra with exceeding probabilities equal to 81%, 63%, 10% and 5% provided by Italian seismic code highlighting the values of S_a[g] related to the fundamental periods of the four base-isolated structural models. As proposed and discussed by [17], with the aim to consider the abovementioned uncertainty within the design life, four Gaussian PDFs of the lnS_a[g] random variable, represented in Fig. 4, corresponding to the fundamental periods of the four base-isolated structural models have been assumed and the corresponding mean (E[$lnS_a(T_{is})$[g]]) and coefficient of variation (COV) values have been defined by fitting the above-discussed exceeding probabilities related to the 4 limit states provided by NTC08 [29] for each isolated period.

Table 5
Selected ground motion records characteristics [67].

	Earthquake	Date	M	Fault mechanism	R (km)	EC8 site class	Waveform ID	Earthquake ID
GM1	Bingol	05/01/2003	6.3	Strike-slip	11.79	B	209	38
GM2	Christchurch	06/13/2011	6	Reverse	5.1	A	386	149
GM3	Darfield	09/03/2010	7.1	Strike-slip	13.31	C	330	137
GM4	E Off Izu Peninsula	05/03/1998	5.5	Reverse	9.5	B	153	59
GM5	EMILIA_Pianura_Padana	05/29/2012	6	Reverse	4.73	C	313	133
GM6	Friuli 4th shock	09/15/1976	5.9	Reverse	16.83	B	429	75
GM7	Hector mine	10/16/1999	7.1	Strike-slip	28.61	B	412	35
GM8	Honshu	08/10/1996	5.9	Reverse	13.89	B	56	21
GM9	Hyogo - Ken Nanbu	01/16/1995	6.9	Strike-slip	16.6	C	306	34
GM10	Landers	06/28/1992	7.3	Strike-slip	13.08	B	457	98
GM11	L'Aquila mainshock	04/06/2009	6.3	Normal	5.65	B	167	64
GM12	Loma Prieta	10/18/1989	6.9	Oblique	27.59	B	456	94
GM13	Mid Niigata prefecture	10/23/2004	6.6	Reverse	16.42	C	41	16
GM14	MT FUJI REGION	03/15/2011	5.9	Strike-slip	12.8	B	285	125
GM15	N Miyagi prefecture	07/25/2003	6.1	Reverse	9.93	C	34	15
GM16	Northridge	01/17/1994	6.7	Reverse	20.19	C	459	99
GM17	Off Noto Peninsula	03/25/2007	6.7	Reverse	6.64	B	136	50
GM18	Olfus	05/29/2008	6.3	Strike-slip	8.25	A	218	101
GM19	Rumoi	12/14/2004	5.7	Reverse	8.08	B	47	18
GM20	South Iceland	06/17/2000	6.5	Strike-slip	5.25	A	113	41
GM21	Southern Iwate prefecture	06/13/2008	6.9	Reverse	23.08	B	139	51
GM22	W Tottori prefecture	10/06/2000	6.6	Strike-slip	11.78	B	20	12

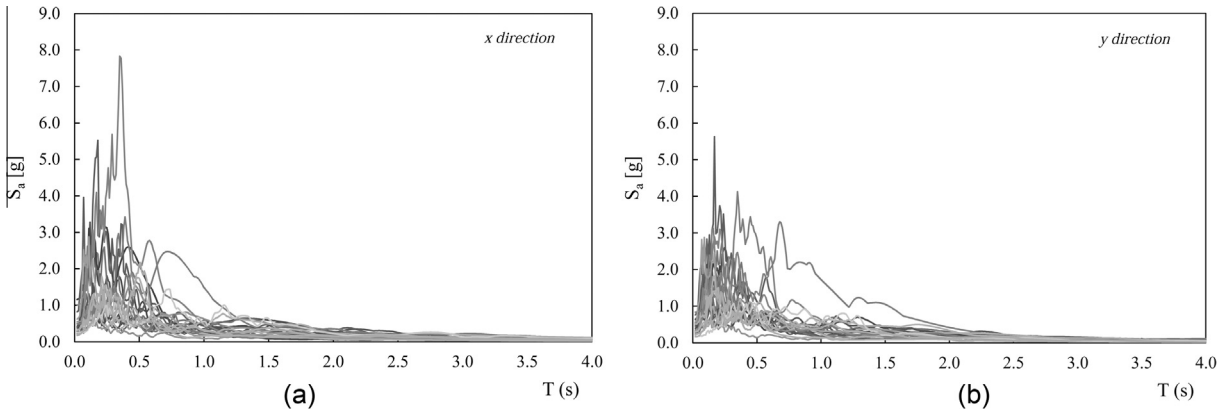

Fig. 5. Pseudo-acceleration spectra (ξ_{is} = 2%) of the selected real ground motion records: x direction (a); y direction (b).

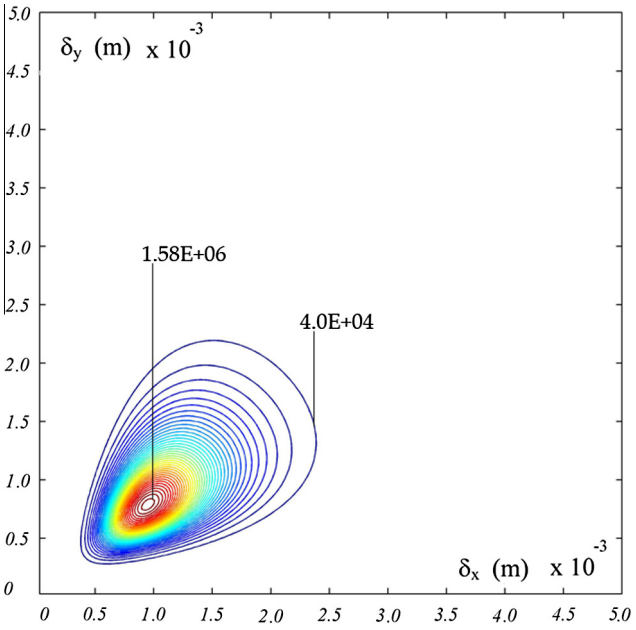

Fig. 6. Contour lines of the lognormal bivariate (joint) probability density function (substructure level, I_d = 4.5, R = 1.5 m).

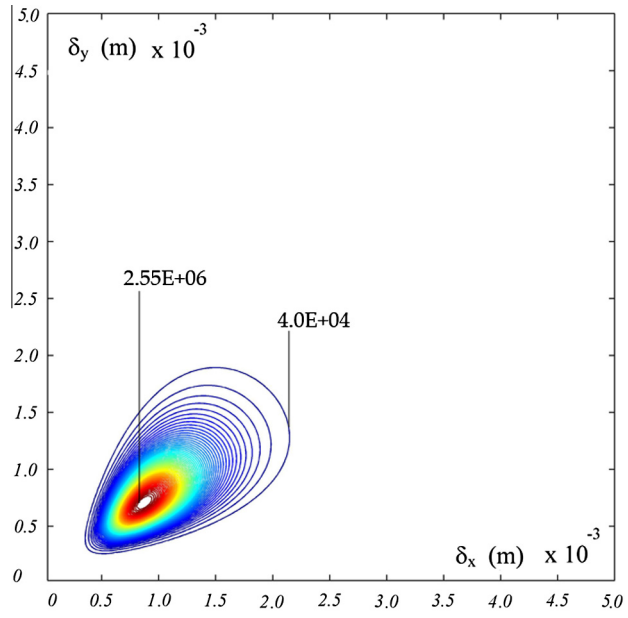

Fig. 7. Contour lines of the lognormal bivariate (joint) probability density function (substructure level, I_d = 5.3, R = 2.0 m).

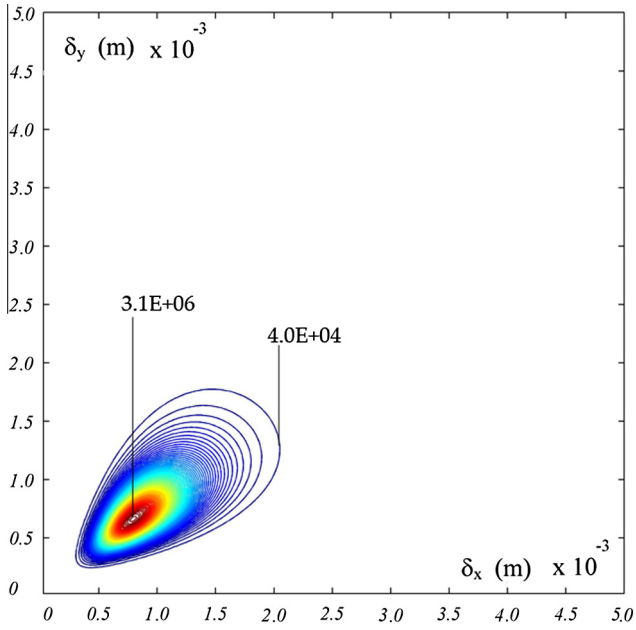

Fig. 8. Contour lines of the lognormal bivariate (joint) probability density function (substructure level, I_d = 6.4, R = 3.0 m).

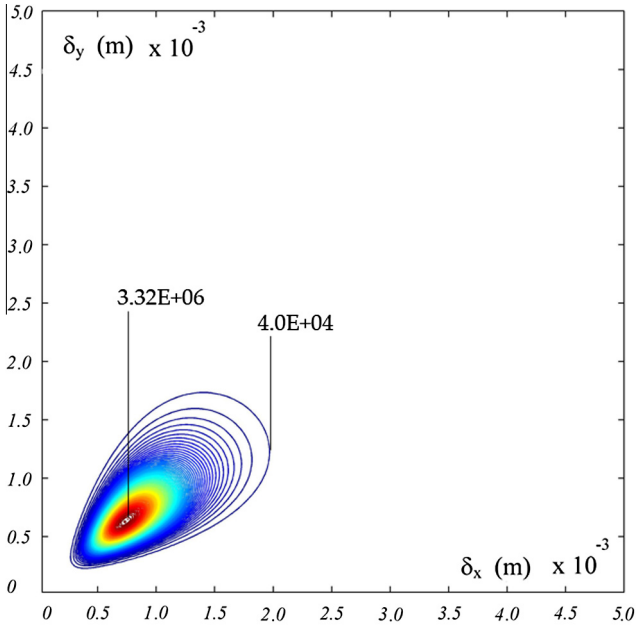

Fig. 9. Contour lines of the lognormal bivariate (joint) probability density function (substructure level, I_d = 7.4, R = 4.0 m).

Starting from the probability density functions of the two random variables, the Latin Hypercube sampling (LHS) method, developed by McKey et al. [33], widely employed in many literature works [34–36], has been used to generate the input data samples of the structural models by sampling 22 values from each PDF and perform the non-linear dynamic analyses. More details about the definition of the input data samples may be found in [17].

Unscaled real records with the three components have been selected from the European Strong-Motion Database [67] by matching the 22 spectral accelerations S_a of the ground motions, regarding each T_{is}, with the values sampled from each PDF of the S_a random variable. The characteristics of the selected ground motion records are listed in Table 5.

Fig. 5(a) and (b) shows the acceleration spectra (ξ_{is} = 2%) of the selected unscaled real earthquake excitations for x and y directions, respectively.

4. Seismic reliability evaluation

With the aim to evaluate the seismic safety of the superstructure and substructure and to define SRBD abacuses and equations useful to design the FP system, inelastic response-history analyses have been carried out in SAP2000 [54] on the statistical samples of each structural model. A total number of 484 building samples has

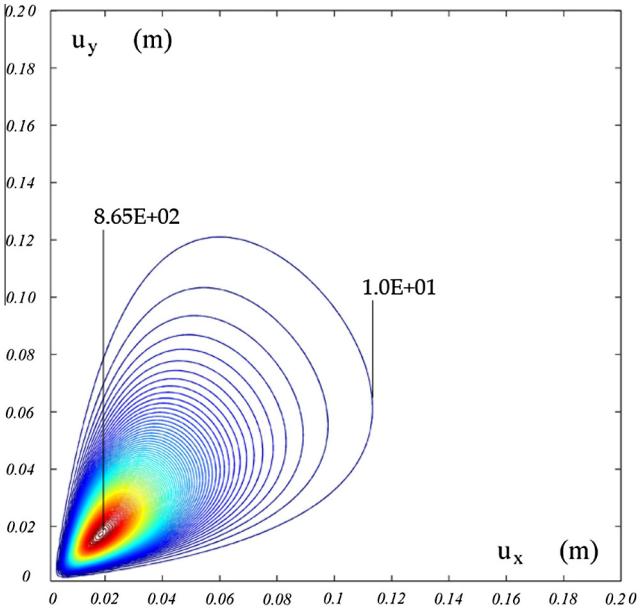

Fig. 10. Contour lines of the lognormal bivariate (joint) probability density function (isolation level, I_d = 4.5, R = 1.5 m).

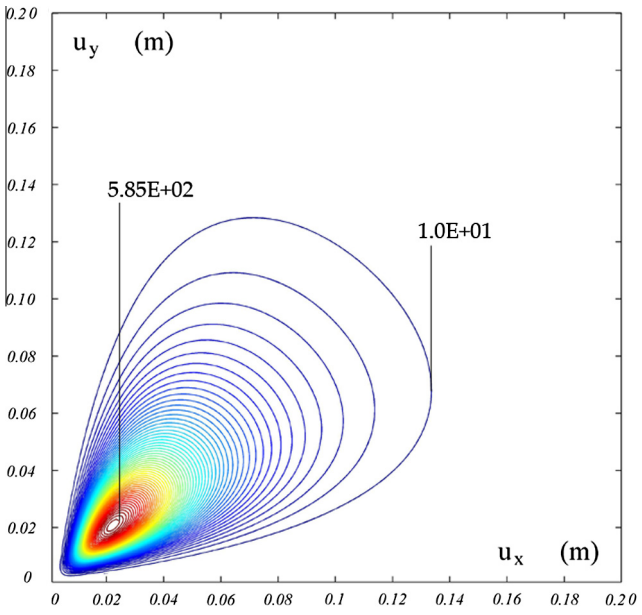

Fig. 11. Contour lines of the lognormal bivariate (joint) probability density function (isolation level, I_d = 5.3, R = 2.0 m).

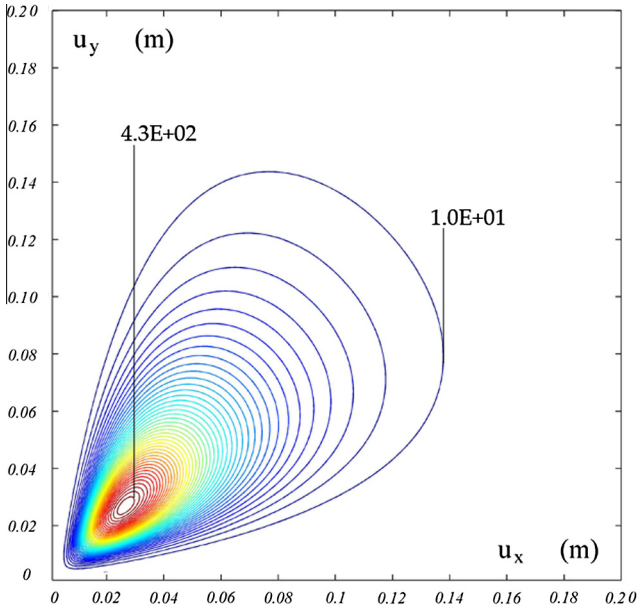

Fig. 12. Contour lines of the lognormal bivariate (joint) probability density function (isolation level, I_d = 6.4, R = 3.0 m).

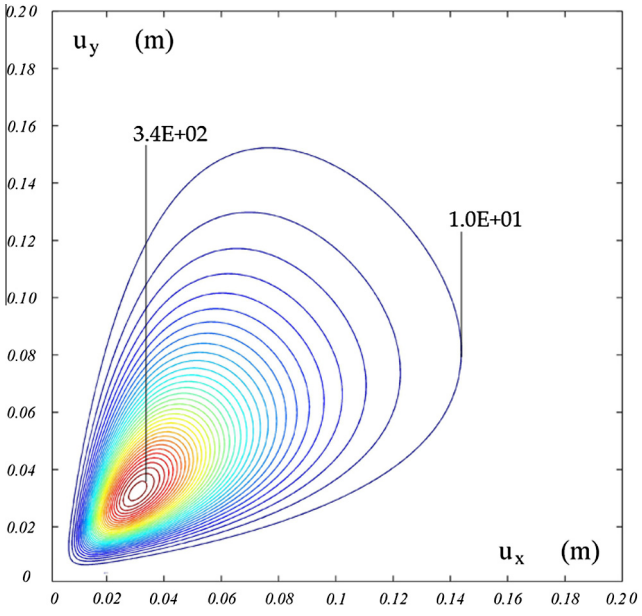

Fig. 13. Contour lines of the lognormal bivariate (joint) probability density function (isolation level, I_d = 7.4, R = 4.0 m).

been generated for each of the four different configurations of the base-isolated building model (T_{is} = 2.58 s, T_{is} = 2.85 s, T_{is} = 3.47 s, T_{is} = 4.01 s) for a total number of 1936 non-linear dynamic analyses.

As regards an angle column, the absolute maximum interstory drifts, δ_x and δ_y, at each level of the superstructure and substructure as well as the absolute maximum isolator relative displacements, u_x and u_y, have been evaluated for each simulation in both directions. The abovementioned response parameters are assumed as engineering demand parameters (EDPs) according to the performance-based seismic design and to follow a lognormal distribution. This probabilistic model is widely employed in Probabilistic Based Earthquake Engineering (PBEE) [68] and in many studies concerning the performance of structural systems similar to that considered in this work [14,17].

On the above-described results and using the maximum likelihood estimation method, the mean and standard deviation of both the absolute maximum interstory drift and the absolute maximum horizontal relative isolator displacement along each direction (x and y directions) have been estimated. As discussed in [17], the three-dimensional effects and correlations between the plane response parameters are not negligible with the consequence that the seismic reliability estimation has to be based on the bivariate exceeding probabilities. It follows that considering the displacements in both directions as dependent and correlated variables and estimating the matrix of correlation coefficients, lognormal bivariate (joint) probability density functions (JPDFs) have been

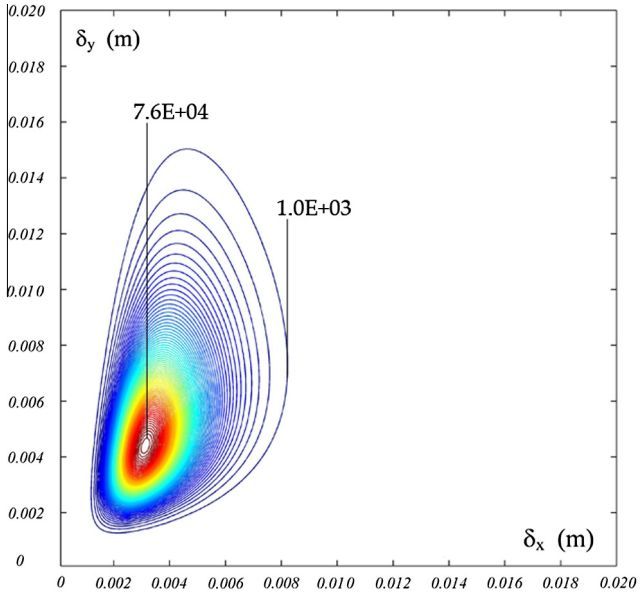

Fig. 14. Contour lines of the lognormal bivariate (joint) probability density function (superstructure 1st level, I_d = 4.5, R = 1.5 m).

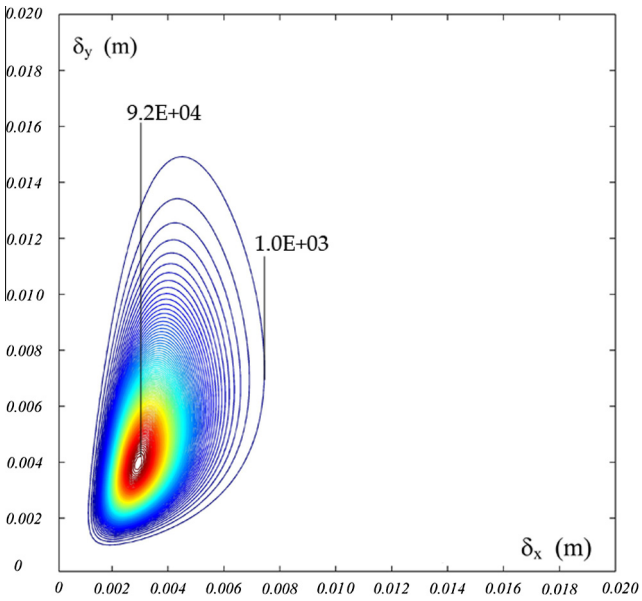

Fig. 15. Contour lines of the lognormal bivariate (joint) probability density function (superstructure 1st level, I_d = 5.3, R = 2.0 m).

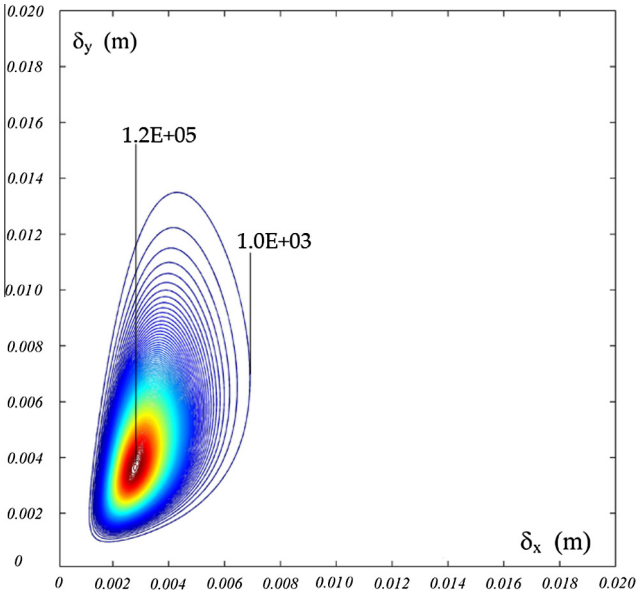

Fig. 16. Contour lines of the lognormal bivariate (joint) probability density function (superstructure 1st level, I_d = 6.4, R = 3.0 m).

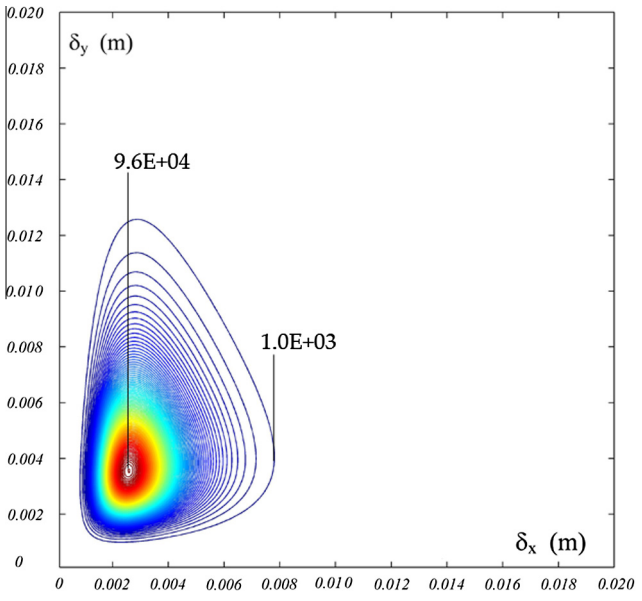

Fig. 17. Contour lines of the lognormal bivariate (joint) probability density function (superstructure 1st level, I_d = 7.4, R = 4.0 m).

evaluated. The corresponding JPDFs related to the substructure, isolation level and the first story of the superstructure are respectively shown in Figs. 6–17 as contour lines for each value of the isolation degree I_d.

The mean and dispersion values of the JPDFs related to the substructure and superstructure 1st level generally decrease for increasing the isolation degree, whereas the statistical parameters of the JPDFs related to the isolation level increase for higher isolated periods.

Considering different limit state domains defined on the bi-directional displacements, the seismic reliability of the overall system has been evaluated. In particular, the different limit state functions (performance objectives PO) have been defined in terms of interstory drift (IDI: Interstory Drift Index) [51], reduced according both to FEMA-274 and NTC08 provisions, and isolation relative displacement in order to estimate the exceeding bivariate probabilities P_f. The volumes delimited by the joint probability density functions and limit state domains assumed, consisting of cylindrical functions representative of the limit IDIs for superstructure and substructure and of the relative displacements for isolation level in both directions, have been numerically evaluated to estimate the no-exceeding bivariate probabilities. Then, the exceeding bivariate probabilities, defined as the bivariate complementary cumulative distribution functions (CCDFs), have been evaluated by calculating the complementary values of the no-exceeding bivariate probabilities. A generic lognormal joint probability density function with generic limit state domains is illustrated in Fig. 18. Figs. 19–22 show the comparison between the (bivariate) SP curves, plotted in logarithmic scale, of the 4th,

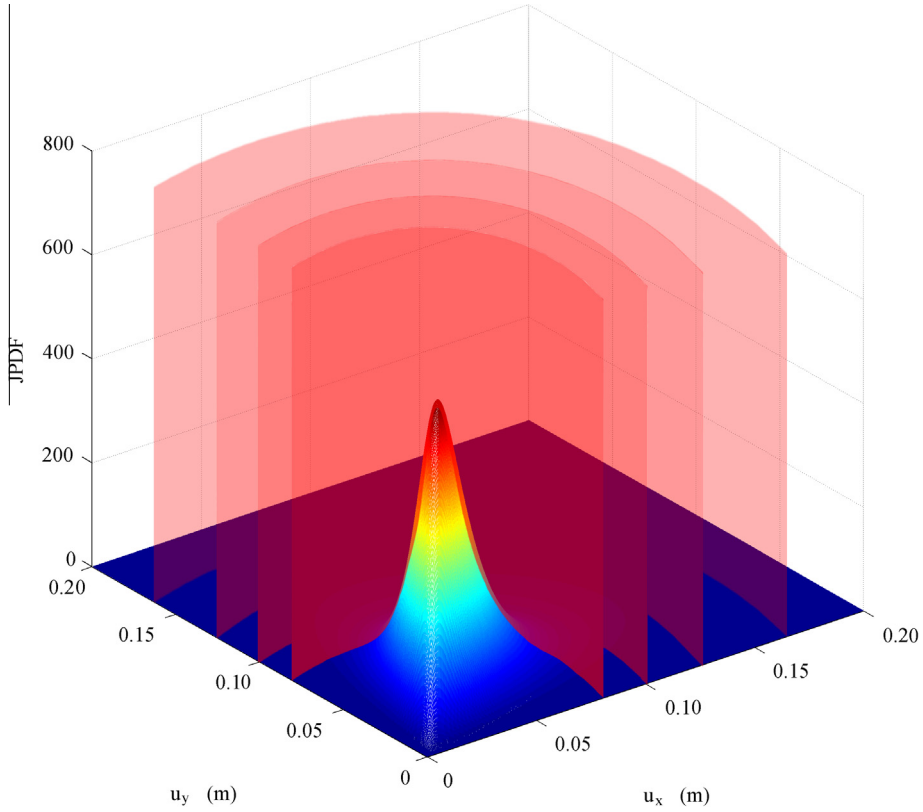

Fig. 18. Generic lognormal bivariate (joint) probability density function with generic cylindrical limit state domains.

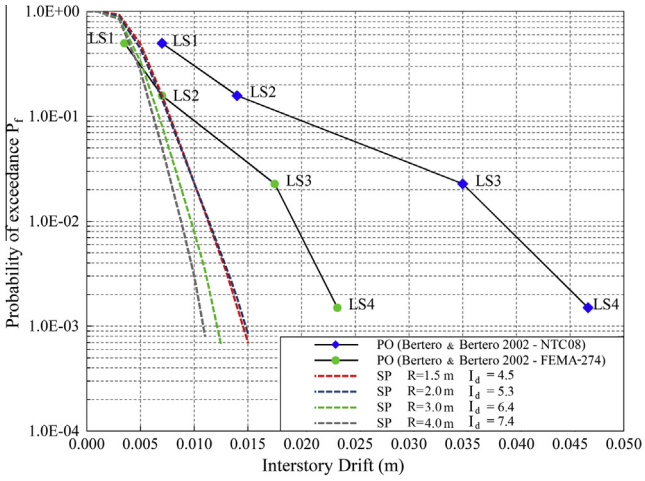

Fig. 19. Exceeding bivariate probabilities at 4th story (SP curves) compared to PO curves, for the four different values of the isolation degree I_d.

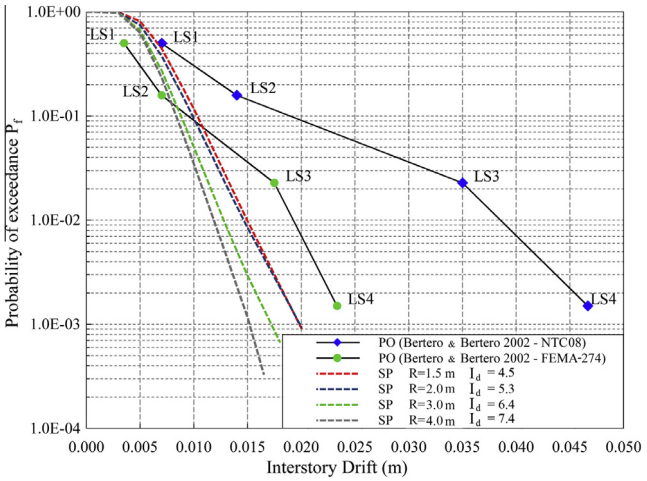

Fig. 20. Exceeding bivariate probabilities at 3rd story (SP curves) compared to PO curves, for the four different values of the isolation degree I_d.

3rd and 2nd levels (superstructure) and 1st level (substructure), obtained for the different I_d values, against the PO curves defined as described in section 3. Seismic reliability for each level of the superstructure and substructure increases (lower exceeding probabilities) with increasing of the isolation degree, as shown in Figs. 19–22, but some limit states are violated due to both the uncertainty characterizing the friction coefficient and the vertical components of the seismic excitations.

Fig. 19 presents the (bivariate) SP curves of the top level of the superstructure. Referring to the more restrictive PO curve defined according to FEMA-274 provisions, the *LS1* is violated for any value of the isolation degree I_d varying in the range of interest. It follows that even with an isolation degree $I_d = 7.4$, (radius of curvature $R = 4.0$ m), concrete cracks (corresponding to slight damage state, *LS1*) at the roof level elements probably occur. Adopting an isolation degree $I_d \geqslant 6.4$ ($R \geqslant 3.0$ m) the damage on secondary elements (corresponding to moderate damage state, *LS2*) may be prevented. Referring to the PO curve defined according to NTC08 provisions, no damage should be expected even for the lowest isolation degree I_d considered.

In Figs. 20 and 21, the (bivariate) SP curves of the first two levels of the superstructure are represented. Referring to the PO curve defined according to FEMA-274 provisions, the SP curves related to lower values of the isolation degree $I_d = 4.5$ and $I_d = 5.3$,

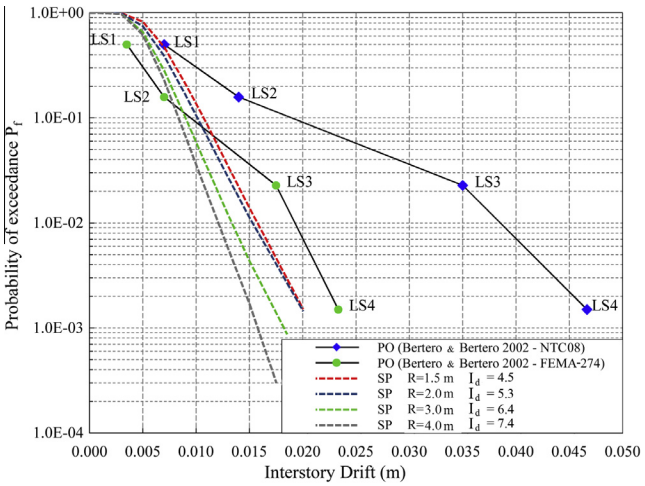

Fig. 21. Exceeding bivariate probabilities at 2nd story (SP curves) compared to PO curves, for the four different values of the isolation degree I_d.

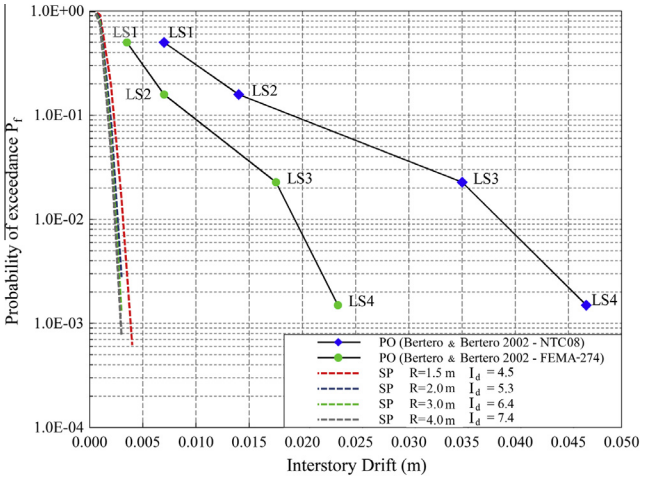

Fig. 22. Exceeding bivariate probabilities at 1st story (SP curves) compared to PO curves, for the different values of the isolation degree I_d.

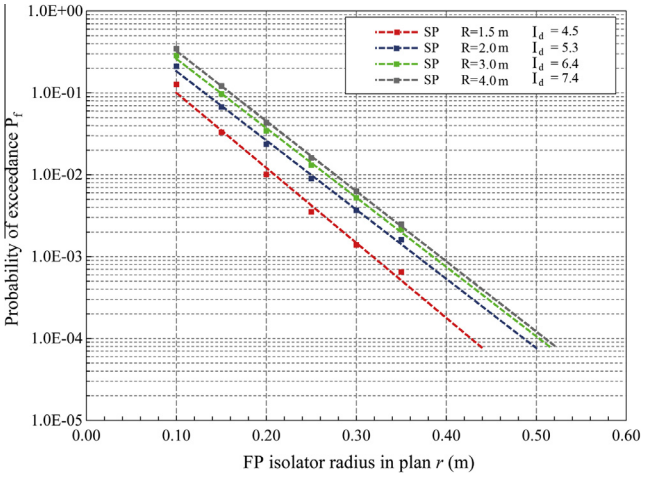

Fig. 23. Exponential regression curves related to the exceeding bivariate probabilities at the isolation level for different values of the isolation degree I_d.

Table 6
Structure limit state dependent cost calculations.

Limit state	C_1	C_2	C_3	C_4	C_5	C_6	C_7	$C^i_{LS,s,Sum}$
LS1	3.8E+04	1.3E+04	2.0E+03	3.4E+04	6.1E+00	8.2E+00	2.9E+02	8.8E+04
LS2	1.5E+05	5.1E+04	7.6E+03	1.3E+05	6.1E+01	8.2E+01	2.9E+03	3.4E+05
LS3	3.5E+05	1.2E+05	2.1E+04	3.6E+05	6.1E+02	8.2E+02	2.9E+04	8.7E+05
LS4	7.7E+05	2.6E+05	6.1E+04	1.0E+06	8.2E+03	8.2E+04	5.7E+06	7.9E+06

(R = 1.5 m and R = 2.0 m respectively), plenty exceed the first two limit state *LS1* and *LS2*. Neither adopting I_d = 7.4 (R = 4.0 m), damage on the secondary elements can be prevented. With reference to the PO curve defined according to NTC08 provisions, the *LS1* is reached for the lowest isolation degree I_d = 4.5 (R = 1.5 m).

The results related to the isolation degree I_d = 4.5 (R = 1.5 m) are consistent with the results obtained in [17], in which the behaviour of the superstructure is considered linear, due to the value of the post-yield stiffness ratio.

The plan dimension of the single-concave isolators (i.e. radius in plan r of the concave surface) can be designed from the (bivariate) structural performance curves of the isolation level, ($SP_{isolator}$) depicted in Fig. 23, as also proposed in [17], with the aim to respect an expected reliability level. The exponential regression curves of the isolation system related to the exceeding bivariate probabilities for different displacement domains are plotted in Fig. 23 for the different isolation degrees I_d of interest. The regression equations are evaluated in the probability range of interest between 1.0E−01 and 1.0E−03 for displacements varying from 0.10 m to 0.60 m. The R-square values are higher than 0.99 for all the proposed seismic reliability-based design (SRBD) equations. The regression curves show that for a given (bivariate) exceeding probability P_f, a higher value of the radius in plan r is required as the isolation degree I_d increases. Therefore, an exceeding probability of $P_f = 1.5 \cdot 10^{-3}$ (related to the collapse limit state, reliability index β = 3 in 50 years) is achievable, for I_d = 4.5 (R = 1.5 m), with a radius in plan r = 0.30 m; whereas in the case of I_d = 7.4 (R = 4.0 m), the same reliability level is achieved with a higher value of r equal to about 0.40 m. The equations of the exponential regression bivariate structural performance curves of the FP system for increasing values of the isolation degree I_d apply respectively:

$$P_f = 0.825\exp(-21.10r) \quad (11)$$

$$P_f = 1.289\exp(-19.47r) \quad (12)$$

$$P_f = 1.839\exp(-19.52r) \quad (13)$$

$$P_f = 2.343\exp(-19.73r) \quad (14)$$

where P_f is the exceeding probability and r (meter) is the radius in plan of the FP isolator.

The SRBD abacus and derived equations are useful to design FP bearing devices, having a radius of curvature ranging from R = 1.5 m to R = 4.0 m, for symmetrical buildings in an area with a seismic hazard similar to that considered.

5. Life-cycle cost assessment

In this section, the results obtained from the life-cycle cost analysis (LCCA) applied to the four different models of the base-isolated system and referred to both FEMA-274 and NTC08 perfor-

Table 7
Limit states dependent costs and initial cost.

	Limit state	$C^i_{LS,\,Sum}\,P_i$							
		FEMA-274				NTC08			
		I_d = 4.5	I_d = 5.3	I_d = 6.4	I_d = 7.4	I_d = 4.5	I_d = 5.3	I_d = 6.4	I_d = 7.4
Superstructure	*LS1*	1.68E+04	1.48E+04	1.18E+04	1.13E+04	2.67E+03	2.29E+03	1.39E+03	1.03E+03
	LS2	1.06E+04	9.13E+03	5.50E+03	4.06E+03	2.47E+02	1.96E+02	7.65E+01	3.58E+01
	LS3	9.33E+01	7.11E+01	2.27E+01	8.55E+00	1.05E−02	6.39E−03	6.72E−04	7.78E−05
	LS4	5.03E+01	3.56E+01	8.00E+00	2.06E+00	2.22E−04	1.17E−04	5.81E−06	3.10E−07
	$\sum C^i_{LS}\,P_i$	2.76E+04	2.40E+04	1.74E+04	1.54E+04	2.92E+03	2.49E+03	1.47E+03	1.07E+03
	$\frac{\nu}{\lambda}(1-e^{-\lambda t})$	18.36							
	C_{LS}	5.07E+05	4.41E+05	3.19E+05	2.82E+05	5.35E+04	4.57E+04	2.69E+04	1.96E+04
Substructure	*LS1*	2.140E+01	6.211E+00	2.886E+00	1.773E+00	7.802E−03	6.289E−04	1.355E−04	5.031E−05
	LS2	3.048E−02	2.457E−03	5.295E−04	1.966E−04	4.068E−09	3.801E−11	0.000E+00	0.000E+00
	LS3	0.000E+00	0.000E+00	0.000E+00	0.000E+00	0.000E+00	0.000E+00	0.000E+00	0.000E+00
	LS4	0.000E+00	0.000E+00	0.000E+00	0.000E+00	0.000E+00	0.000E+00	0.000E+00	0.000E+00
	$\sum C^i_{LS}\,P_i$	2.143E+01	6.213E+00	2.886E+00	1.773E+00	7.802E−03	6.289E−04	1.355E−04	5.031E−05
	$\frac{\nu}{\lambda}(1-e^{-\lambda t})$	18.36							
	C_{LS}	3.93E+02	1.14E+02	5.30E+01	3.26E+01	1.43E−01	1.15E−02	2.49E−03	9.24E−04
	C_{IN}	3.3E+05	3.4E+05	3.5E+05	3.5E+05	3.3E+05	3.4E+05	3.5E+05	3.5E+05

mance objectives are presented and compared. The purpose is to evaluate the influence of the isolation degree I_d on both the initial costs and the economic losses due to future earthquakes for the considered structure and location.

The LCCA has been applied considering the PO curves defined according to both FEMA-274 and NTC08 provisions. Table 6 summarizes the four limit state dependent cost values based on the calculation formulas of Table 1.

In order to obtain the present value of the limit states dependent cost $C_{LS}(t,\boldsymbol{s})$ of Eq. (1), the annual exceedance probabilities of the interstory drifts related to each limit state are required. According to [38], the values of the annual exceeding probability $P_{t=1}(\Delta > \Delta_i)$ in Eq. (6), for each level of the superstructure, substructure and isolation level and for each isolation degree (I_d = 4.5, I_d = 5.3, I_d = 6.4, I_d = 7.4) are obtained starting from the bivariate SP curves, illustrated in Figs. 19–23, and transforming the design-life (50 years) exceeding probabilities into annual exceeding probabilities according to Poisson's model, Eq. (15):

$$P_{t=1} = -\frac{1}{50}\ln(1-P_f) \tag{15}$$

and, then, substituting $P_{t=1}$ in Eqs. (4)–(3) to calculate the limit states dependent cost for the superstructure and substructure. In Table 7, the limit states dependent costs calculated through Eq. (3) are reported. The difference between the values obtained regarding FEMA-274 and NTC08 is high for the superstructure due to the lower values of the limit state thresholds provided by FEMA274, and increases for the substructure level because of the very low values of the exceeding probabilities.

The limit states dependent cost associated with the isolation devices, special maintenance cost $C_{LS,d}$, has been estimated, for each structural models (*SM*) configuration, using Eqs. (2), (3), where t is the service life of the devices, i = 1 is the number of limit states considered, $\Delta = r$ is the limit state threshold, taking into account that r is the maximum displacement capability of the devices, designed selecting the radius in plan of the concave surface for an exceeding probability $P_f = 1.5\cdot 10^{-3}$ in 50 years ($SP_{isolator}$ curves of Fig. 23).

The results obtained from the LCCA for the different isolation degrees and for the both seismic code provisions are shown in Fig. 24(a) and (b). In particular, the initial costs C_{IN}, the expected limit states dependent costs $C_{LS}(t,\ \boldsymbol{s})$ and the total life-cycle costs C_{TOT} of the four base-isolated models are illustrated.

From these results, it is possible to observe that the major difference in terms of the total life-cycle cost between the four isolation degrees is given by the limit state dependent cost $C_{LS}(t,\boldsymbol{s})$. The initial construction costs C_{IN} are independent of the limit state

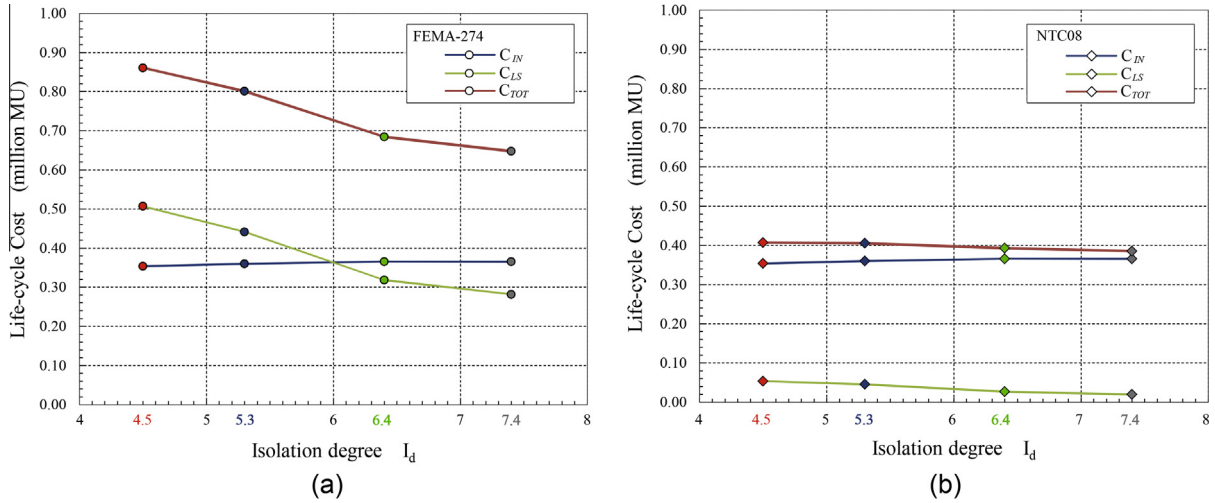

Fig. 24. Total life-cycle cost of the BI system for different values of the isolation degree I_d, regarding the PO curves of FEMA-274 (a) and NTC08 (b).

exceeding probabilities and increase of about 3% from I_d = 4.5 to 7.4 because of the initial and regular maintenance costs of the isolation devices in the worst case of their replacement every 10 years assumed in the analysis.

From Fig. 24(a), where the limit states dependent costs of superstructure and substructure have been evaluated with reference to the more restrictive FEMA-274 performance objectives, it is possible to note that (i) the limit states dependent cost associated with the low values of the isolation degree highly overcomes the initial construction cost of the building; (ii) an isolation degree I_d = 7.4 allows to reduce the expected limit states dependent cost of about 55% if compared to the case with an isolation degree equal to I_d = 4.5; (iii) higher values of the isolation degree lead to lower values of the total life-cycle cost demonstrating the effectiveness of the isolation degree for the r.c. building considered.

In Fig. 24(b) the limit states dependent cost of the superstructure and substructure have been evaluated with reference to the less restrictive NTC08 performance objectives. In this case: (i) the limit states dependent cost is a fraction of the construction cost for all the values of the isolation degree adopted due to the very low annual exceeding probabilities of the limit states; (ii) higher values of the isolation degree always lead to lower values of the total life-cycle cost.

6. Conclusions

The purpose of this study is to evaluate the influence of the isolation degree on the seismic reliability and life-cycle costs of an ordinary 3D base-isolated r.c. structure through single-concave FP isolators with a design life of 50 years and located near L'Aquila site (Italy), considering both earthquake main characteristics and isolator properties as the random variables relevant to the problem. Several 3D non-linear dynamic analyses have been performed in order to evaluate the system response considering both the vertical and horizontal components of each seismic excitation. Bivariate (joint) probability density functions have been computed and, assuming the limit state domains (performance objectives), the bivariate exceeding probabilities (structural performances) have been estimated in order to compare SP to PO curves.

The results from the seismic reliability analysis of the considered system, designed according to NTC08 and FEMA-274, indicate that the seismic reliability of the superstructure and substructure improves as isolation degree increases and that some limit states are violated due to both the uncertainty characterizing the friction coefficient and the vertical components of the seismic excitations.

The structural performance curves of the isolation level, ($SP_{isolator}$) or the proposed equations can be used to design the plan dimension of the isolator (i.e. radius in plan r of the concave surface) in order to respect reliability levels depending on the isolation degree. In particular, an exceeding probability of $P_f = 1.5 \cdot 10^{-3}$ (related to the collapse limit state, reliability index β = 3 in 50 years) is achievable, for I_d = 4.5 (R = 1.5 m), with a radius in plan $r = 0.3$ m; whereas in the case of I_d = 7.4 (R = 4.0 m), the same reliability level is achieved with a higher value of r equal to about 0.40 m. The seismic reliability-based design (SRBD) abacuses and derived equations, proposed in this study, can be used to design the FP bearing devices, having a radius of curvature R ranging from 1.5 m to 4.0 m, employed to seismically isolate regular buildings located in an area characterized by a seismic hazard similar to that considered.

Finally, from the results of the life-cycle cost analysis, it is possible to note that (i) the initial cost of the four base-isolated models is similar (about 3% variation); (ii) the major difference in terms of total life-cycle cost between the four isolation degrees is given by the limit states dependent cost especially regarding the more restrictive FEMA-274 performance objectives: in particular an isolation degree I_d = 7.4 allows to reduce the expected limit states dependent cost of about 55% if compared to the case of an isolation degree equal to I_d = 4.5; (iii) higher values of the isolation degree lead to lower values of the total life-cycle cost demonstrating the effectiveness of the isolation degree for the r.c. building considered.

References

[1] Christopoulos C, Filiatrault A. Principles of passive supplemental damping and seismic isolation. Pavia, Italy: IUSS Press; 2006.
[2] Zayas VA, Low SS, Mahin SA. A simple pendulum technique for achieving seismic isolation. Earthq Spectra 1990;6:317–33.
[3] Jangid RS. Optimum frictional elements in sliding isolation systems. Comput Struct 2000;76:651–61.
[4] Chen Y, Ahmadi G. Stochastic earthquake response of secondary systems in base-isolated structures. Earthq Eng Struct Dynam 1992;21:1039–57.
[5] Chen Y, Ahmadi G. Wind effects on base-isolated structures. J Eng Mech ASCE 1992;118:1708–27.
[6] Lin YK, Cai GQ. Probabilistic structural dynamics—advanced theory and applications. NY: McGraw-Hill; 1995.
[7] Chen J, Liu W, Peng Y, Li J. Stochastic seismic response and reliability analysis of base-isolated structures. J Earthq Eng 2007;11:903–24.
[8] Fan FG, Ahmadi G. Random response analysis of frictional base isolation system. J Eng Mech 1990;116(9):1881–901.
[9] Su L, Ahmadi G. Response of frictional base isolation systems to horizontal–vertical random earthquake excitations. Probab Eng Mech 1988;3(1):12–21.
[10] Alhan C, Gavin HP. Reliability of base isolation for the protection of critical equipment from earthquake hazards. Eng Struct 2005;27:1435–49.
[11] Zou XK, Wang Q, Li G, Chan CM. Integrated reliability-based seismic drift design optimization of base-isolated concrete buildings. J Struct Eng 2010;136:1282–95.
[12] Mishra SK, Roy BK, Chakraborty S. Reliability-based-design-optimization of base isolated buildings considering stochastic system parameters subjected to random earthquakes. Int J Mech Sci 2013;75:123–33.
[13] Zhao C, Chen J. Numerical simulation and investigation of the base isolated NPPC building under three-directional seismic loading. Nucl Eng Des 2013;265:484–96.
[14] Castaldo P, Tubaldi E. Influence of fps bearing properties on the seismic performance of base-isolated structures. Earthq Eng Struct Dynam 2015;44:2817–36.
[15] Palazzo B, Castaldo P, Della Vecchia P. Seismic reliability analysis of base-isolated structures with friction pendulum system. In: 2014 IEEE workshop on environmental, energy and structural monitoring systems proceedings Napoli September 17–18.
[16] Palazzo B, Castaldo P, Della Vecchia P. Seismic reliability of base-isolated structures with friction pendulum isolators (FPS). In: 2nd European conference on earthquake engineering and seismology, Istanbul August 25–29.
[17] Castaldo P, Palazzo B, Della Vecchia P. Seismic reliability of base-isolated structures with friction pendulum bearings. Eng Struct 2015;95:80–93.
[18] Cornell CA, Krawinkler H. Progress and challenges in seismic performance assessment. PEERCenter News 2000;4(1):1–3.
[19] Ang AH-S, Lee J-C. Cost optimal design of RC buildings. Reliab Eng Syst Saf 2001;73:233–8.
[20] Esteva L, Díaz-Lòpez O, García Pérez J, Sierra G, Ismael E. Life-cycle optimization in the establishment of performance-acceptance parameters for seismic design. Struct Saf 2002;24(2–4):187–204.
[21] Ang AH-S, Leon DD. Determination of optimal target reliabilities for design and upgrading of structures. Struct Saf 1997;19(1):91–103.
[22] García-Pérez J. Seismic zoning for initial- and total-cost minimization. Earthq Eng Struct Dynam 2000;29:847–65.
[23] García-Pérez J, Zenteno M, Díaz O. Vulnerability functions and the influence of seismic design parameters on initial costs for buildings provided with hysteretic energy-dissipating devices. Earthq Resistant Eng Struct 2007;93 (VI):3–12. http://dx.doi.org/10.2495/ERES070011.
[24] Castaldo P, De Iuliis M. Optimal integrated seismic design of structural and viscoelastic bracing-damper systems. Earthq Eng Struct Dynam 2014;43 (12):1809–27.
[25] Castaldo P. Integrated seismic design of structure and control systems. New York: Springer International Publishing; 2014.
[26] Park K-S, Koh H-M, Hahm D. Integrated optimum design of viscoelastically damped structural systems. Eng Struct 2004;26:581–91.
[27] Palazzo B. Seismic behavior of base-isolated buildings. In: Proceedings of the international meeting on earthquake protection of buildings.
[28] Naeim F, Kelly JM. Design of seismic isolated structures: from theory to practice. John Wiley & Sons Inc; 1999.
[29] NTC08. Norme tecniche per le costruzioni. Gazzetta Ufficiale del 04.02.08, DM 14.01.08. Ministero delle Infrastrutture.
[30] Constantinou MC, Whittaker AS, Kalpakidis Y, Fenz DM, Warn GP. Performance of seismic isolation hardware under service and seismic loading. Technical report MCEER-07-0012; 2007.

[31] Constantinou MC, Mokha A, Reinhorn AM. Teflon bearings in base isolation. II: Modeling. J Struct Eng 1990;116(2):455–74.
[32] Mokha A, Constantinou MC, Reinhorn AM. Teflon bearings in base isolation. I: Testing. J Struct Eng 1990;116(2):438–54.
[33] Mckey MD, Conover WJ, Beckman RJ. A comparison of three methods for selecting values of input variables in the analysis from a computer code. Technometrics 1979;21:239–45.
[34] Dolsek M. Incremental dynamic analysis with consideration of modelling uncertainties. Earthq Eng Struct Dynam 2009;38:805–25.
[35] Vořechovský M, Novák D. Correlation control in small-sample Monte Carlo type simulations I: a simulated annealing approach. Probab Eng Mech 2009;24 (3):452–62.
[36] Celarec D, Dolšek M. The impact of modelling uncertainties on the seismic performance assessment of reinforced concrete frame buildings. Eng Struct 2013;52:340–54.
[37] Wen YK, Kang YJ. Minimum building life-cycle cost design criteria I: methodology. J Struct Eng 2001;127(3):330–7.
[38] Mitripoulou ChCh, Lagaros ND, Papadrakakis M. Life-cycle cost assessment of optimally designed reinforced concrete buildings under seismic actions. Reliab Eng Struct Saf 2011;96:1330–1.
[39] Shin H, Singh MP. Minimum failure cost-based energy dissipation system design for buildings in three seismic regions – part I: elements of failure cost analysis. Eng Struct 2014;74:266–74.
[40] Clemente P, Buffarini G. Seismic isolation and protection systems. Base isolation: design and optimization criteria. J Anti-Seismic Syst Int Soc (ASSISi) 2010;1(1).
[41] SEAOC-Vision 2000 Committee. Vision 2000-a framework for performance-based earthquake engineering, vol. 1. Sacramento (CA): Structural Engineers Association of California; 1995.
[42] FEMA-350. Recommended seismic design criteria for new steel moment-frame buildings. Washington, DC: Federal Emergency Management Agency; 2000.
[43] Ghobarah A. On drift limits associated with different damage levels. In: Proceedings of the international workshop on performance-based seismic design; June 28–July 1.
[44] FEMA-227. A benefit-cost model the seismic rehabilitation of buildings. Washington, DC: Federal Emergency Management Agency, Building Seismic Safety Council; 1992.
[45] ATC-13. Earthquake damage evaluation data for California. Redwood City, CA: Applied Technology Council; 1985.
[46] CEN – European Committee for Standardization. Eurocode 0: basis of structural design. Final draft. Brussels; 2006.
[47] Building Seismic Safety Council. NEHRP commentary on the guidelines for the seismic rehabilitation of buildings. Provisions (FEMA-274). Washington, DC; 1997.
[48] Collins KR, Stojadinovic B. Limit states for performance-based design. 12WCEE; 2000.
[49] Aoki Y, Ohashi Y, Fujitani H, Saito T, Kanda J, Emoto T, Kohno M. Target seismic performance levels in structural design for buildings. 12WCEE; 2000.
[50] Saito T, Kanda J, Kani N. Seismic reliability estimate of building structures designed according to the current Japanese design code. In: Proceedings of the structural engineers world congress.
[51] Bertero RD, Bertero VV. Performance-based seismic engineering: the need for a reliable conceptual comprehensive approach. Earthq Eng Struct Dynam 2002;31:627–52. http://dx.doi.org/10.1002/eqe.146.
[52] Almazàn JL, De la Llera JC. Physical model for dynamic analysis of structures with FPS isolators. Earthq Eng Struct Dynam 2003;32:1157–84. http://dx.doi.org/10.1002/eqe.266.
[53] Kilar V, Koren D. Seismic behaviour of asymmetric base isolated structures with various distributions of isolators. Eng Struct 2009;31:910–21.
[54] SAP 2000. Computers and Structures Inc.: Berkley, CA; 2002.
[55] Zayas VA, Low SS, Mahin SA. The FPS earthquake resisting system Report No. CB/EERC-87/01. Berkeley, California: Earthquake Engineering Research Center, University of California; 1987.
[56] Park YJ, Wen YK, Ang AHS. Random vibration of hysteretic systems under bi-directional ground motions. Earthq Eng Struct Dynam 1986;14:543–57.
[57] Nagarajaiah S, Reinhorn AM, Constantinou MC. 3D-basis: non linear dynamic analysis of three-dimensional base isolated structures: Part II. Technical report NCEER-91-0005; 1991.
[58] Tena-Colunga A, Escamilla-Cruz JL. Torsional amplifications in asymmetric base-isolated structures. Eng Struct 2007;29(2):237–47.
[59] FEMA-356. Prestandard and commentary for the seismic rehabilitation of buildings. Washington, DC: Federal Emergency Management Agency; 2000.
[60] Ripani M, Etse G, Vrech S, Mroginski J. Thermodynamic gradient-based poroplastic theory for concrete under high temperatures. Int J Plast 2014;61:157–77.
[61] Etse G, Vrech SM, Ripani M. Constitutive theory for Recycled Aggregate Concretes subjected to high temperature. Constr Build Mater 2016;111:43–53.
[62] Kulkarni JA, Jangid RS. Effects of superstructure flexibility on the response of base-isolated structures. Shock Vib 2003;26:1–13.
[63] Cornell CA. Engineering seismic risk analysis. Bull Seismol Soc Am 1968;58 (5):1583–606.
[64] Bazzurro P, Cornell CA. Disaggregation of seismic hazard. Bull Seismol Soc Am 1999;89:501–20.
[65] Shome N, Cornell CA, Bazzurro P, Carballo JE. Earthquake, records, and nonlinear responses. Earthq Spectra 1998;14(3):469–500.
[66] Luco N, Cornell CA. Structure-specific scalar intensity measures for near-source and ordinary earthquake ground motions. Earthq Spectra 2007;23 (2):357–92.
[67] ESMD <http://www.isesd.hi.is/>.
[68] Aslani H, Miranda E. Probability-based seismic response analysis. Eng Struct 2005;27(8):1151–63.